

25. S. Chakrabati, K. Brechling, B. Moss, *Mol. Cell. Biol.* **5**, 3403 (1985).
26. I. Bacik, J. H. Cox, R. Anderson, J. W. Yewdell, J. R. Bennink, *J. Immunol.* **152**, 381 (1994).
27. J. M. Lambert, P. D. Senter, A. Yau-Young, W. A. Blättler, V. S. Goldmacher, *J. Biol. Chem.* **260**, 12035 (1985).
28. We thank L. Van Kaer, P. Ashton-Rickarts, and S. Tonegawa (Massachusetts Institute of Technology, Cambridge, MA) for TAP1 knockout mice, J. Yewdell and J. Bennink [National Institutes of Health (NIH)] for

the vaccinia minigene construct, B. Benacerraf for helpful discussions, and M. Michalek (Dana-Farber Cancer Institute, Boston, MA) for the MF2.2D9 T-T hybrid. Supported by grants AI20248 and AI31337 from NIH. M.K.-B. is a recipient of a fellowship from the Swiss National Science Foundation. The care and use of animals was in accordance with the guidelines of the Dana-Farber Cancer Institute and NIH.

9 August 1994; accepted 21 November 1994

## Requirement of FGF-4 for Postimplantation Mouse Development

Benjamin Feldman, William Poueymirou,  
Virginia E. Papaioannou, Thomas M. DeChiara,  
Mitchell Goldfarb\*

Fibroblast growth factors (FGFs) are thought to influence many processes in vertebrate development because of their diverse sites of expression and wide range of biological activities in in vitro culture systems. As a means of elucidating embryonic functions of FGF-4, gene targeting was used to generate mice harboring a disrupted *Fgf4* gene. Embryos homozygous for the null allele underwent uterine implantation and induced uterine decidualization but did not develop substantially thereafter. As was consistent with their behavior in vivo, *Fgf4* null embryos cultured in vitro displayed severely impaired proliferation of the inner cell mass, whereas growth and differentiation of the inner cell mass were rescued when null embryos were cultured in the presence of FGF-4 protein.

Polypeptide ligands mediate intercellular communication governing cell growth, differentiation, and patterning in the vertebrate embryo. Ligands essential for normal embryogenesis from gastrulation onward include insulin-like growth factors, platelet-derived growth factor, mast cell growth factor, WNT-1, and FGFs (1–3). Although several ligands, such as FGFs and transforming growth factors  $\alpha$  and  $\beta$ , are expressed in embryos before gastrulation (4–7), only maternally expressed leukemia inhibitory factor is known to provide an essential function by mediating uterine implantation of the blastocyst (8). By generating mice deficient for FGF-4, we show that embryonically expressed FGF-4 is required for postimplantation development of embryos in vivo and for normal inner cell mass (ICM) proliferation in vitro.

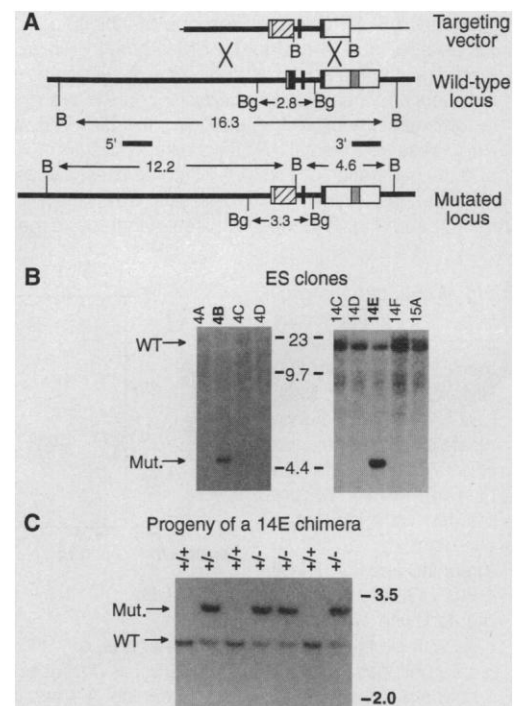
FGFs are a family of nine structurally related ligands (9) that can activate a cor-

responding family of receptor tyrosine kinases (10) to elicit a wide range of cellular responses. The 21-kD FGF-4 protein (11) is mitogenic toward cultured fibroblasts,

melanoblasts, endothelial cells, and embryonic limb mesenchyme (12, 13) and induces mesoderm formation in amphibian ectoderm explants (14). The *Fgf4* gene is expressed in undifferentiated embryonic stem (ES) cells and their oncogenic equivalent, embryonal carcinoma (EC) cells (15), and this expression is governed by an evolutionarily conserved 3' enhancer element (16). In order to achieve a high frequency of *Fgf4* gene disruption in ES cells, we used an "enhancerless" targeting vector (17) with a promoterless neomycin-resistance gene downstream from a 5' homology segment bearing the native *Fgf4* promoter and upstream from a 3' homology segment lacking the enhancer (Fig. 1A). Homologous recombination of the vector into the *Fgf4* locus deletes exon 1, which encodes the first 109 amino acids of FGF-4, including the NH<sub>2</sub>-terminal secretion signal sequence (18). When this vector was electroporated into ES cells (19), 3 out of 80 G418-resistant ES clones examined showed homologous recombination at the *Fgf4* locus. Two of these clones, 4B and 14E (Fig. 1B), were microinjected into blastocysts to yield chimeric mice that were able to transmit the mutant allele through the germ line (Fig. 1C) (20). Unexpectedly, the 14E ES line had lost the Y chromosome and transmitted the mutant allele through female chimeras only (21).

Heterozygous males and females were phenotypically normal and fertile. Inter-crosses between heterozygotes failed to yield

**Fig. 1.** Strategy of *Fgf4* disruption. **(A)** Targeting vector (17), the *Fgf4* locus (18), and the mutated *Fgf4* locus. The targeting vector is aligned above the wild-type allele to illustrate the homologous recombination event that generated the disrupted allele, depicted below. The disrupted allele lacks the first 109 codons of *Fgf4*, which encode the NH<sub>2</sub>-terminal secretion signal and the first 28 residues of the FGF family core homology region. Shown are the *Fgf4* coding sequence (filled boxes), the 3' enhancer (16) (gray box), other untranslated regions of *Fgf4* exons (open boxes), the Neo<sup>r</sup> coding sequence (hatched box), the genomic sequence (thick line), the vector sequence (thin line), the upstream Xba I-Eco RI probe (5'), the downstream Pvu II-Sal I probe (3'), Bam HI (B), and Bgl II (Bg). **(B)** Southern blot analysis of DNA from ES clones. The 3' probe hybridizes to a diagnostic 4.6-kbp fragment (in addition to the wild-type 16.3-kbp fragment) in Bam HI-digested DNA from targeted clones 4B and 14E. WT, wild-type band; mut., mutant band. Detection of expected 12.2- and 16.3-kbp Bam HI fragments with the 5' probe confirmed homologous recombination on both sides of the targeting vector (27). **(C)** Southern blots of DNA from progeny of 14E-derived chimeras. Bgl II-digested DNAs from litters were probed with a mixture of Neo<sup>r</sup> and exon 1 fragments, which detect diagnostic 3.3- and 2.8-kbp fragments, respectively (20).



B. Feldman, Integrated Program in Cellular, Molecular, and Biophysical Studies, Columbia University College of Physicians and Surgeons, 701 West 168 Street, New York, NY 10032, USA, and Regeneron Pharmaceuticals Inc., 777 Old Saw Mill River Road, Tarrytown, NY 10591, USA.

W. Poueymirou, T. M. DeChiara, M. Goldfarb, Regeneron Pharmaceuticals, Inc., 777 Old Saw Mill River Road, Tarrytown, NY 10591, USA.

V. E. Papaioannou, Department of Genetics and Development, Columbia University College of Physicians and Surgeons, 701 West 168 Street, New York, NY 10032, USA.

\*To whom correspondence should be addressed.

offspring homozygous for the *Fgf4* null allele (Table 1). Because 29 of the progeny were from intercrosses between 14E-derived and 4B-derived heterozygotes, the lack of *Fgf4* null progeny cannot be due to homozygosity of an undetected linked mutation inadvertently generated in either of the targeted ES

cell lines. We conclude that homozygosity for the *Fgf4* null allele is lethal during embryonic development.

The *Fgf4* gene is embryonically expressed in several sites, first in the morula, the embryonic component (the ICM) of the blastocyst, and the embryonic ectoderm

of the postimplantation egg cylinder (5, 22), then later in primitive dorsal mesoderm, embryonic epithelia, muscle, and tooth mesenchyme (5, 6). As many of these expression sites might be required for development to birth, we examined embryos from heterozygote intercrosses at several different days of gestation (Table 1).

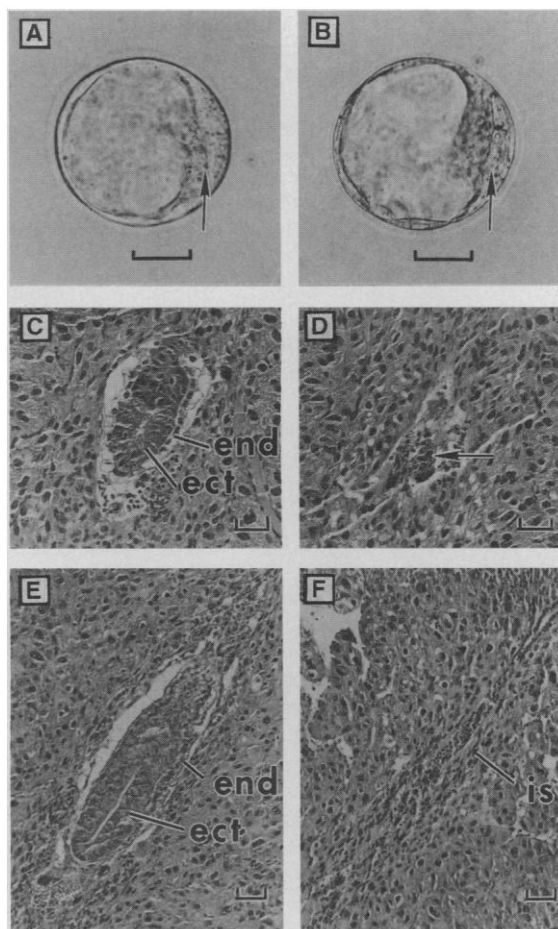
Among 121 phenotypically normal E3.5 (3.5 days of gestation) blastocysts, 30 (25%) were homozygous for the mutant allele (Table 1 and Fig. 2, A and B), which indicates that FGF-4 is not essential for embryogenesis before uterine implantation. At E8.5 (the mid-somite stage), all decida were externally indistinguishable, but dissection revealed that 12 out of 38 (32%) implantation sites lacked discernible embryos, yolk sacs, or ectoplacental cones. Of 20 phenotypically normal E8.5 embryos subjected to genotyping, none were homozygous mutants (Table 1). As was consistent with these data, none of 21 phenotypically normal E14.5 embryos were homozygous mutants, whereas an additional seven implantation sites (25% of total) were undergoing resorption (Table 1). Histological examination of E5.5 and E6.5 serially sectioned decida was used to further define the onset of defects in *Fgf4* null embryos. On E5.5, 24 to 36 hours after implantation, a majority of the embryos had a normal egg cylinder appearance, bearing a layer of extraembryonic endoderm surrounding the embryonic ectoderm (Fig. 2C). However, 4 of 20 (20%) implantation sites had a small disorganized (Fig. 2D) or undetectable embryonic component (Table 1). On E6.5, 11 of 45 (24%) decida contained apparent embryo implantation sites bearing necrotic cells but lacking discernible embryonic structures (Fig. 2F and Table 1). The high frequency of abortive postimplantation development (legend to Table 1) and lack of older *Fgf4* null embryos demonstrate that *Fgf4* null embryos degenerate shortly after uterine implantation.

Given the expression of FGF receptors in the perimplantation embryo (22) and maternal deciduum (23), the abortive development of *Fgf4* mutant embryos could result from defects intrinsic to the embryo or could result exclusively from the breakdown in signaling between embryo and uterus. To explore these alternatives, we assessed in vitro growth of blastocysts (24) from heterozygote intercrosses. Thirty-five blastocysts were individually cultured for 5 days, then photographed and lysed for genotyping. Although cultured blastocysts of each genotype (*Fgf4*<sup>+/+</sup>, *Fgf4*<sup>+/-</sup>, and *Fgf4*<sup>-/-</sup>) (Fig. 3, A and B) gave rise to an adherent sheet of trophoblast-like cells (Fig. 3, C and D), including trophoblastic giant cells (Fig. 3E), *Fgf4*<sup>-/-</sup> blastocysts showed severely impaired proliferation of the ICM. As

**Table 1.** *Fgf4* genotypes and phenotypes of embryos and neonates derived from heterozygote intercrosses. All neonates as well as E14.5 and E8.5 embryos were genotyped as either +/- or +/+. The probabilities of not observing -/- genotypes by sampling variability are indicated in the right-hand column (28). The abnormal phenotypes at E8.5 (normal deciduum lacking embryo) or E14.5 (resorption sites) are inferred to be the consequence of the homozygous null genotype. E6.5 decida lacked discernible embryos in 11 of 45 cases, and E5.5 decida had defective or undiscernible embryos in 4 of 20 cases, which are inferred to be the consequence of the null genotype on the basis of the far lower frequency of decida lacking embryos among control matings (28). Twenty-five percent of phenotypically normal E3.5 blastocysts were *Fgf4*<sup>-/-</sup>. As is observed among embryos from wild-type matings, a fraction of E3.5 embryos from the heterozygote intercrosses appeared abnormal but were not significantly biased to the null genotype (see numbers in parentheses). Neonates and E14.5 embryos were genotyped by Southern blot (20), whereas E8.5 and E3.5 embryos were genotyped by PCR (29).

Stage	Phenotypes		Genotypes of normal embryos and neonates			P value
	Normal	Abnormal	<i>Fgf4</i> <sup>+/+</sup>	<i>Fgf4</i> <sup>+/-</sup>	<i>Fgf4</i> <sup>-/-</sup>	
Neonate	59	0	17	42	0	<0.005
E14.5	21	7	5	16	0	<0.01
E8.5	26	12	7	13	0	<0.01
E6.5	34	11	-	-	-	<0.005
E5.5	16	4	-	-	-	<0.025
E3.5	121	(15)	24 (1)	67 (9)	30 (5)	>0.5

**Fig. 2.** Phenotypes of mutant embryos. (A) *Fgf4*<sup>+/-</sup> blastocyst. (B) *Fgf4*<sup>-/-</sup> blastocyst, morphologically normal (arrows point to ICM). (C) Section through phenotypically normal E5.5 egg cylinder, showing embryonic ectoderm (ect) and extraembryonic endoderm (end). (D) Section through small defective E5.5 egg cylinder bearing few embryonic cells (arrow) associated with the *Fgf4* null genotype (see Table 1 legend). (E) Section through an E6.5 deciduum showing a phenotypically normal egg cylinder. (F) Section through an E6.5 deciduum showing a typical degenerated implantation site (is) associated with the null genotype (see legend to Table 1). Decida were fixed, paraffin embedded, serially sectioned, and stained with hematoxylin and eosin. E3.5 blastocysts were collected from heterozygote intercrosses; photographed (with phase contrast optics); lysed in 10- $\mu$ l lysis buffer [500 mM KCl, 100 mM tris-HCl (pH 8), gelatin (0.1 mg/ml), 0.45% NP-40, 0.45% Tween-20, and proteinase K (0.5 mg/ml)]; wax overlaid (Ampliwax PCR gems; Perkin-Elmer); incubated at 60°C for 3 min, at 55°C for 4 hours, and at 100°C for 10 min; and subjected to PCR analysis (29). Scale bar: 20  $\mu$ m in (A) and (B); 50  $\mu$ m in (C) through (F).



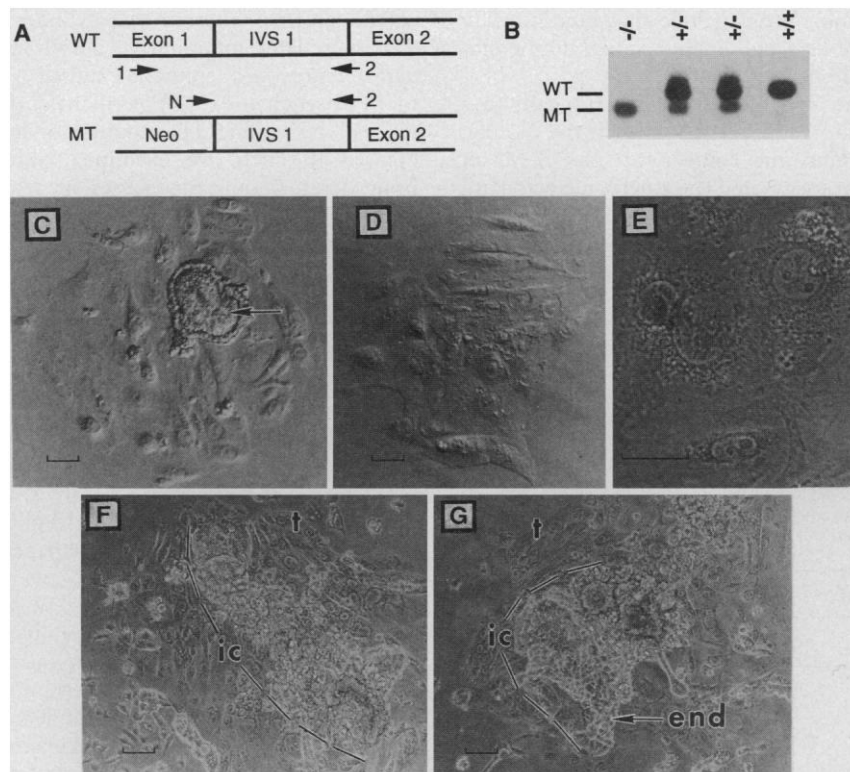


**Fig. 3.** Genotypes and phenotypes of blastocyst and rescued morula outgrowths. Blastocysts (E3.5) were cultured for 5 days on gelatin-coated microwells (3 cm in diameter) in Dulbecco's modified Eagle's medium plus 15% fetal bovine serum, supplemented with glutamine, antibiotics, and 0.1 mM 2-mercaptoethanol (24); followed by photography, lysis, and genotyping. Alternatively, morulae (E2.5) were freed from their zone pellucidae and cultured for 7 days in medium supplemented with FGF-4 (100 ng/ml) and heparin (1  $\mu$ g/ml) followed by photography, lysis, and genotyping. (A) Scheme for PCR detection of wild-type and mutant *Fgf4* alleles. (B) Sample genotypes of blastocyst outgrowths obtained by Southern blot analysis of PCR reaction products (29). Diagnostic 514-bp wild-type (WT) and 420-bp mutant (MT) bands are indicated. (C) In vitro outgrowth from an *Fgf4*<sup>+/-</sup> blastocyst, illustrating an ICM (arrow) with an outer layer of extraembryonic endoderm (Hoffman optics). (D) Outgrowth from an *Fgf4*<sup>-/-</sup> blastocyst, lacking ICM or endoderm. (E) Phase-contrast, high magnification image of an *Fgf4*<sup>-/-</sup> outgrowth, showing trophoblast giant cells with large nuclei, pronounced nucleoli, and perinuclear granules. *Fgf4*<sup>+/-</sup> (F) and *Fgf4*<sup>-/-</sup> (G) morulae cultured in the presence of FGF-4, showing in phase-contrast trophoblasts (t), ICM (ic), and endodermal cells (end). All *Fgf4*<sup>-/-</sup> genotypes from blastocyst and morula outgrowths were confirmed in three or more independent PCR reactions. Scale bar, 20  $\mu$ m.

summarized in Fig. 4, the null genotype was never associated with robust outgrowths of the ICM (as in Fig. 3C) and was the only genotype associated with undetectable ICM outgrowth (as in Fig. 3D).

In a separate experiment, in which 23 morulae (E2.5) derived from heterozygote intercrosses were cultured in vitro and monitored daily, all embryos developed normally to the expanded blastocyst stage, but the ICM in all four *Fgf4*<sup>-/-</sup> embryos slowly regressed (21). By contrast, when recombinant human FGF-4 protein was included in the medium of 49 cultured morulae, proliferation of the ICM was rescued in 100% (12 total) of *Fgf4*<sup>-/-</sup> embryos. Some of the FGF-4-treated wild-type and null embryos (Fig. 3, F and G) displayed substantial ICM proliferation and differentiation to extraembryonic endoderm, a phenomenon previously observed in FGF-4-treated ICM cultures (22). The developmental defects of *Fgf4* null embryos in vivo and in vitro dem-

onstrate that FGF-4 serves as an autocrine or paracrine ligand promoting survival and growth of the ICM in the postimplantation phase of development.

In contrast to FGF-4's essential embryonic function, FGF-3 and FGF-5 do not provide functions necessary for embryonic or postnatal viability (3, 25). The embryonic expression of these factors may be expendable because of local coexpression of other ligands, including FGF-4. FGF-4 and FGF-5 are coexpressed in the embryonic ectoderm of the egg cylinder, whereas FGF-4 and FGF-3 are coexpressed in the late gastrula primitive streak, presomitic paraxial mesoderm, and pharyngeal pouch endoderm (7).

In addition to its earliest function, FGF-4 may play critical roles in later stages of development. For example, FGF-4 is thought to act as a natural inducer of limb mesenchyme proliferation, on the basis of its expression in limb apical ectoderm (5, 6) and

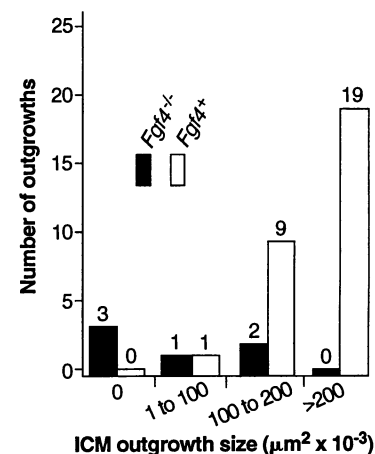


**Fig. 4.** Histogram summary of blastocyst outgrowths. *Fgf4* null and *Fgf4* positive (one or two wild-type alleles) blastocyst cultures are divided into four groups on the basis of the size of their ICM outgrowths after 5 days of culture. The shapes of ICM outgrowths were approximated as ellipses in order to measure surface area.

the mitogenic effects of recombinant FGF-4 applied to cultured limb explants (13, 26). FGF-4 may also participate in mesoderm formation, as suggested by its activity on amphibian ectoderm explants (14) and its expression in the late primitive streak of mice (5, 6). Rescue of the early lethality suffered by *Fgf4* null embryos by means of exogenous factor, transgene expression, or chimerism could provide insights into other embryonic functions of FGF-4.

## REFERENCES AND NOTES

1. J. K. Heath and V. Valancius-Mangel, *Curr. Opin. Cell Biol.* **3**, 935 (1991); J.-P. Liu, J. Baker, A. S. Perkins, E. J. Robertson, A. Efstradiatis, *Cell* **75**, 59 (1993); S. Werner *et al.*, *EMBO J.* **12**, 2635 (1993).
2. A. P. McMahon and A. Bradley, *Cell* **62**, 1073 (1990).
3. S. L. Mansour, J. M. Goddard, M. R. Capecchi, *Development* **117**, 13 (1993).
4. G. A. Schultz and S. Heyner, *Oxf. Rev. Reprod. Biol.* **15**, 43 (1993).
5. L. Niswander and G. R. Martin, *Development* **114**, 755 (1992).
6. B. Drucker and M. Goldfarb, *Mech. Dev.* **40**, 155 (1993).
7. D. G. Wilkinson, G. Peters, C. Dickson, A. P. McMahon, *EMBO J.* **7**, 691 (1988); O. Haub and M. Goldfarb, *Development* **112**, 397 (1991); J. M. Hébert, M. Boyle, G. R. Martin, *ibid.*, p. 407.
8. C. L. Stewart *et al.*, *Nature* **359**, 76 (1992).
9. M. Goldfarb, *Cell Growth Differ.* **1**, 439 (1990); A. Tanaka *et al.*, *Proc. Natl. Acad. Sci. U.S.A.* **89**, 8928 (1992); M. Miyamoto *et al.*, *Mol. Cell. Biol.* **13**, 4251 (1993).
10. D. E. Johnson and L. T. Williams, *Adv. Cancer Res.* **60**, 1 (1993).
11. M. Taira *et al.*, *Proc. Natl. Acad. Sci. U.S.A.* **84**, 2980 (1987); P. Delli-Bovi *et al.*, *Cell* **50**, 729 (1987).
12. P. Delli-Bovi *et al.*, *Mol. Cell. Biol.* **8**, 2933 (1988); K. Miyagawa *et al.*, *Oncogene* **3**, 383 (1988); R. Halaban, B. S. Kwon, S. Ghosh, P. Delli-Bovi, A. Baird, *Oncogene Res.* **3**, 177 (1988).
13. L. Niswander and G. R. Martin, *Nature* **361**, 68 (1993).
14. G. D. Paterno, L. L. Gillespie, M. S. Dixon, J. M. W. Slack, J. K. Heath, *Development* **106**, 79 (1989).
15. A. Velcich, P. Delli-Bovi, A. Mansukhani, E. B. Ziff, C.

Basilico, *Oncogene Res.* **5**, 31 (1989); J. K. Heath, G. D. Paterno, A. C. Lindon, D. R. Edwards, *Development* **107**, 11 (1989); J. Tiesman and A. Rizzino, *In Vitro Cell. Dev. Biol.* **25**, 1193 (1989).

16. A. M. Curatola and C. Basilico, *Mol. Cell. Biol.* **10**, 2475 (1990).

17. The targeting vector was constructed by modification of pMC1neo-polyA+ (Stratagene) with the use of segments of a C57BL/6 *Fgf4* genomic clone (6) and strategies based on published restriction maps and sequences (18): 5' homology segment 4.25-kbp Sac I-Sac II genomic fragment including the transcriptional promoter and 105 bases of the 5' untranslated region; Neo<sup>r</sup> coding sequence, 1.0-kbp Mlu I-Bam HI segment lacking the polyoma virus promoter; and 3' homology segment, 2.2-kbp Bss HII-Pvu II fragment (converted to Bam HI ends with linkers) extending from intron 1 into 3' untranslated sequence.

18. S. Brookes, R. Smith, J. Thurlow, C. Dickson, G. Peters, *Nucleic Acids Res.* **17**, 4037 (1989).

19. Nde I-linearized vector was electroporated (2) into CB1-4 ES cells [derived from C57BL/6 × Rb(11:16)2H/Rb(16:17)32Lub progeny], and standard procedures were used for G418 selection, DNA extraction, and Southern (DNA) blot hybridization (27).

20. Homologous recombinant ES cells were microinjected into MF1 (Harlan Sprague-Dawley) or C57BL/6 (Taconic Farms) blastocysts and fostered into avertin-anesthetized mice as described (24). Chimeras were crossed with C57BL/6 mice, and DNA was isolated from the tails of the F<sub>1</sub> progeny. Bgl II-digested DNA was hybridized with Neo<sup>r</sup> and exon 1-specific probes generated by polymerase chain reaction (PCR) amplification of cloned wild-type or mutant sequences with oligos immediately upstream (CCACCGTTGCGTC-CCTATT) and downstream (GGAGCTCGACTC-TACTCAG) of the deleted exon. All animal work was done in accordance with federal and New York State guidelines.

21. B. Feldman, W. Poueymirou, V. E. Papaioannou, T. M. DeChiara, M. Goldfarb, data not shown.

22. D. A. Rappolee, C. Basilico, Y. Patel, Z. Werb, *Development* **120**, 2259 (1994).

23. G. Gao and M. Goldfarb, unpublished data.

24. E. J. Robertson, Ed., *Teratocarcinomas and Embryonic Stem Cells: A Practical Approach* (IRL Press, Oxford, 1987).

25. J. M. Hébert, T. Rosenquist, J. Gotz, G. R. Martin, *Cell* **78**, 1017 (1994).

26. L. Niswander and G. R. Martin, *Development* **119**, 287 (1993); A. Vogel and C. Tickle, *ibid.*, p. 199.

27. P. L. Schwartzberg, S. P. Goff, E. J. Robertson, *Science* **246**, 799 (1989).

28. The  $\chi^2$  values for genotype distributions were derived with the use of a null hypothesis predicting 25% *Fgf4*<sup>-/-</sup> embryos. The significance of high-frequency abnormal E5.5 and E6.5 decidua from heterozygote intercrosses was assessed by  $\chi^2$ , with the use of the combined average frequency of abnormal decidua seen in control (4 in 84 amongst *Fgf4*<sup>+/-</sup> × *Fgf4*<sup>+/+</sup> and wild-type progeny) and experimental matings to define null hypothesis abortive development rates of 7.7 and 11.6%, respectively.

29. Lysate (1 to 3  $\mu$ l) was amplified in a 100- $\mu$ l PCR reaction containing 2.5 U of native Pfu DNA polymerase (Stratagene), 20 mM tris-HCl (pH 8.2), 10 mM KCl, 6 mM (NH<sub>4</sub>)<sub>2</sub>SO<sub>4</sub>, 1.5 mM MgCl<sub>2</sub>, 0.1% Triton X-100, 200  $\mu$ M each deoxynucleoside triphosphate, and 50 pmol each of primers 1 (TCAAAGGCTTCG-GCGGCT), 2 (GAGAGCTCCAGAAGACCTG), and N (CGGGTGTGGGTCGTTTGT) with 1 cycle at 97°C for 5 min, 55°C for 5 min, and 75°C for 2 min followed by 40 cycles at 97°C for 30 s, 55°C for 30 s, and 75°C for 2 min. Twenty microliters of each reaction was run on a 1.5% agarose gel, Southern blotted, and hybridized with a 438-base pair (bp) *Fgf4* probe generated by PCR with nested upstream (TACTGCAACGTTGGCATCGGA) and downstream (AAAGCCTAGGTGACCCTGGAC) primers. Control PCR experiments with limiting dilutions of *Fgf4*<sup>+/-</sup> genomic DNA template demonstrated that the sensitivities for detecting null or wild-type alleles are comparable.

30. We thank L. Schleifer for his support of this work. We also thank C. Epstein for providing CB1-4 ES cells; L. Breiman for statistical analyses; J. Griffith for providing oligonucleotides; and B. Galeano, C. Murphy, and D. Mahoney for graphics and photog-

raphy. Supported in part by grants HD27198 and HD21988 from the National Institute of Child Health and Development.

6 July 1994; accepted 14 November 1994

## Inhibition of Ras-Induced Proliferation and Cellular Transformation by p16<sup>INK4</sup>

Manuel Serrano, Enrique Gómez-Lahoz, Ronald A. DePinho, David Beach, Dafna Bar-Sagi\*

The cyclin-dependent kinase 4 (CDK4) regulates progression through the G<sub>1</sub> phase of the cell cycle. The activity of CDK4 is controlled by the opposing effects of the D-type cyclin, an activating subunit, and p16<sup>INK4</sup>, an inhibitory subunit. Ectopic expression of p16<sup>INK4</sup> blocked entry into S phase of the cell cycle induced by oncogenic Ha-Ras, and this block was relieved by coexpression of a catalytically inactive CDK4 mutant. Expression of p16<sup>INK4</sup> suppressed cellular transformation of primary rat embryo fibroblasts by oncogenic Ha-Ras and Myc, but not by Ha-Ras and E1a. Together, these observations provide direct evidence that p16<sup>INK4</sup> can inhibit cell growth.

The CDK4-cyclin D kinase complex promotes progression through the G<sub>1</sub> phase of the cell cycle (1). In normal cells, the retinoblastoma tumor suppressor protein (Rb) regulates cell proliferation by binding and sequestering transcription factors essential for S phase (2). These transcription factors are released at late G<sub>1</sub> by phosphorylation of Rb, thereby allowing cells to enter S phase (2). The main function of the CDK4-cyclin D kinase complexes may be to phosphorylate Rb at late G<sub>1</sub> (3). Indeed, transformed cell lines lacking functional Rb do not require the activity of the CDK4-cyclin D kinase to proliferate, and these cell lines are devoid of CDK4-cyclin D complexes (4). The p16<sup>INK4</sup> protein has been biochemically characterized as a protein that specifically binds to and inhibits CDK4, and thus p16<sup>INK4</sup> may regulate Rb phosphorylation (5). The p16<sup>INK4</sup> protein appears to act as a tumor suppressor protein because the p16<sup>INK4</sup> gene (also called *MTS1*, *CDK4I*, or *CDKN2*) is frequently deleted in tumor cell lines and shows a high frequency of point mutations and small deletions in some tumor cell lines and primary tumors (6).

To examine the effect of p16<sup>INK4</sup> on entry into S phase, we microinjected cultured rat embryo fibroblasts (REF-52) arrested in G<sub>0</sub> by serum starvation with a DNA plasmid encoding activated Ha-Ras

(V12Ras) together with a plasmid encoding human p16<sup>INK4</sup> in either sense (p16<sup>INK4</sup>-s) or antisense (p16<sup>INK4</sup>- $\alpha$ s) orientation relative to the promoter (7). DNA synthesis was monitored 30 hours after injection by immunostaining of 5-bromodeoxyuridine (BrdU) incorporated into newly synthesized DNA (8). Microinjection of a V12Ras expression plasmid either alone or together with the p16<sup>INK4</sup>- $\alpha$ s plasmid stimulated the incorporation of BrdU in ~25% of the injected cells, whereas only 2% of the cells injected with the vector plasmid stained positive for BrdU (Fig. 1, A and B). These results are consistent with the values previously reported for V12Ras-induced mitogenesis in this microinjection assay (9). V12Ras-induced stimulation of DNA synthesis was reduced by 80% upon coinjection of p16<sup>INK4</sup>-s (Fig. 1, A and B). The expression of V12Ras and p16<sup>INK4</sup> in the injected cells was confirmed by double immunofluorescence staining (Fig. 1C) (10). These results indicate that expression of p16<sup>INK4</sup> can prevent V12Ras-induced entry into S phase.

To test the specificity of the inhibition of V12Ras-induced mitogenesis by p16<sup>INK4</sup>, we asked whether the effect of p16<sup>INK4</sup> could be counteracted by coexpression of a catalytically inactive CDK4 mutant. We expected that the exogenous CDK4 mutant might bind p16<sup>INK4</sup> and relieve the p16<sup>INK4</sup>-mediated inhibition of cell growth. The catalytically inactive CDK4 mutant, CDK4-K35M, has a methionine in place of the conserved lysine at position 35 that is probably required for binding to adenosine triphosphate (11). We first analyzed the ability of CDK4-K35M to bind to p16<sup>INK4</sup>. In vitro-translated Cdc2, CDK2, CDK4, and CDK4-K35M proteins were incubated

M. Serrano and D. Beach, Howard Hughes Medical Institute, Cold Spring Harbor Laboratory, P.O. Box 100, Cold Spring Harbor, NY 11724, USA.

E. Gómez-Lahoz and R. A. DePinho, Departments of Microbiology and Immunology and of Medicine, Albert Einstein College of Medicine, 1300 Morris Park Avenue, New York, NY 10461, USA.

D. Bar-Sagi, Cold Spring Harbor Laboratory, P.O. Box 100, Cold Spring Harbor, NY 11724, USA.

\*To whom correspondence should be addressed.